

Role that separatrices and stochastic webs play in quantum dynamics

Go. Torres-Vega, Klaus B. Møller, and A. Zúñiga-Segundo

Departamento de Física, Centro de Investigación y de Estudios Avanzados del IPN, Apartado Postal 14-740, 07000 México, Distrito Federal, Mexico

(Received 12 September 1997)

We numerically analyze the influence of separatrices and stochastic webs on the evolution of quantum wave functions in phase space and we compare our findings with the corresponding classical evolution. We study the dynamics in regular and nonregular systems, namely, in a quartic, the pendulum, and the kicked harmonic oscillator potentials. Regardless of the specific potential, there are common features in the dynamics, some of which are revealed when very small parts of the quantum phase-space densities are analyzed. [S1050-2947(98)04102-X]

PACS number(s): 03.65.-w

I. INTRODUCTION

In previous work [1] we have noticed that the “separatrix” for a discontinuous potential (namely, the step potential) and the stochastic web (for the kicked harmonic oscillator) seem to play an important role in the time evolution of quantum states when the dynamics is analyzed in a quantum phase space. If we define a “separatrix” for a step potential of height V_0 at $q=0$ as the line joining the points $(p, q) = (p_c, 0)$ and $(p, q) = (-p_c, 0)$, where $p_c = \sqrt{2mV_0}$ is the minimum value of the momentum for which a classical particle can cross the step, it was found for short propagation times that the quantum state actually uses this separatrix in its evolution as a road that directs its spread in phase space. A similar behavior was found for the kicked harmonic oscillator. Inspired by these observations, we perform in this paper numerical studies of three model systems, two regular and a nonregular one, in order to find out if the effect of separatrices is a general characteristic of quantum motion. Also, we compare the quantum dynamics with the dynamics of the corresponding classical system. These studies are based on the evolution of classical and quantum phase-space (quasi) probability densities.

Classical phase space is divided by separatrices and stochastic webs into regions in which different types of motion are exhibited. Since classical densities can be discontinuous and follow classical trajectories, they find themselves divided by the separatrix or stochastic web and each of its parts evolves according to the dynamics of the region in phase space in which they lie. As we shall see, quantum systems behave in a different way.

For classical systems, we study the evolution of the initial Gaussian probability density

$$\rho(\Gamma; 0) = \frac{1}{\pi\hbar} e^{-\gamma^2(q-q_0)^2/\hbar - \gamma^{-2}(p-p_0)^2/\hbar}, \quad (1)$$

where $\Gamma = (p, q)$ denotes a point in phase space. This density is centered at (p_0, q_0) and it has a classical width of $\Delta q = \sqrt{q^2 - q_0^2} = \gamma^{-1}(\hbar/2)^{1/2}$ in the coordinate direction and of $\Delta p = \sqrt{p^2 - p_0^2} = \gamma(\hbar/2)^{1/2}$ in the momentum direction, where $f(\Gamma) = \int d\Gamma' f(\Gamma') \rho(\Gamma')$ for any function $f(\Gamma)$. We have

used γ and \hbar as scaling parameters such that the product of the classical widths is $\Delta p \Delta q = \hbar/2$ and the ratio between the widths is controlled by γ . In all our numerical investigations we use dimensionless units, and in these units γ is chosen in such a way ($\gamma=1$) that the density has the same width in the coordinate and the momentum directions.

The classical density evolves on some potential $V(q)$ according to Liouville’s equation

$$\frac{\partial}{\partial t} \rho(\Gamma; t) = - \left[\frac{p}{m} \frac{\partial}{\partial q} + F(q) \frac{\partial}{\partial p} \right] \rho(\Gamma; t), \quad (2)$$

where $F(q) = -dV(q)/dq$ is the force that the ensemble of particles experiences. We propagate this density using the backwards method for the propagation of classical densities with reversible equation of motion described in Refs. [2,3].

For quantum studies, we will make use of a coherent-state phase-space representation as described in Refs. [1,2,4,5] and briefly reviewed below. We find this representation particularly useful for our purpose since, on one hand, it allows the analysis of quantum dynamics in a phase space in terms of wave functions in a similar manner as it is done in, for instance, coordinate space, and, on the other hand, the square magnitude of the phase-space wave function is analogous to the Husimi density [6] which then is a tool for comparing classical and quantum dynamics—formally as well as numerically. For this comparison the Husimi density seems more appropriate than other quantum phase-space densities such as, for instance, the Wigner density [7] because of its closer resemblance to a classical phase-space probability density [8–12].

The rest of this paper is organized as follows. The phase-space representation that we use is briefly reviewed in Sec. II. After this review, we explore the role that separatrices play in classical and quantum dynamics for a quartic potential in Sec. III, the pendulum in Sec. IV, and the kicked harmonic oscillator in Sec. V. We summarize our findings in Sec. VI.

II. A PHASE-SPACE REPRESENTATION OF QUANTUM MECHANICS

In this paper, we make use of a state-vector phase-space representation of nonrelativistic quantum mechanics

[1,2,4,5] in which the operators associated to momentum \hat{P} , coordinate \hat{Q} , and inverse coordinate \hat{Q}^{-1} operators are given by

$$\hat{P} \mapsto \frac{p}{2} - i\hbar \frac{\partial}{\partial q}, \quad \hat{Q} \mapsto \frac{q}{2} + i\hbar \frac{\partial}{\partial p},$$

and

$$\hat{Q}^{-1} \mapsto -\frac{i}{\hbar} e^{ipq/2\hbar} \int dp e^{-ipq/2\hbar}.$$

These operators do not commute with each other but, in fact, satisfy the usual commutation relation $[\hat{Q}, \hat{P}] = i\hbar$. Then, the phase-space Schrödinger equation is given by

$$i\hbar \frac{\partial}{\partial t} \langle \Gamma | \psi \rangle = \left[\frac{1}{2m} \left(\frac{p}{2} - i\hbar \frac{\partial}{\partial q} \right)^2 + V \left(\frac{q}{2} + i\hbar \frac{\partial}{\partial p} \right) \right] \langle \Gamma | \psi \rangle, \quad (3)$$

where $\langle \Gamma | \psi \rangle = \psi(\Gamma; t)$ denotes a time-dependent phase-space wave function. Within this representation one can analyze, formally and numerically, quantum dynamics entirely in a phase space in the same way as it is done in coordinate or abstract representations.

For instance, the finding of eigenvalues and eigenfunctions of the Hamiltonian operator can be done in a similar way as it is done in coordinate representation by analytically solving the eigenvalue problem or by propagating a nonstationary initial phase-space function $\langle \Gamma | \psi_0 \rangle$ and utilizing the standard time-dependent formalism which requires of the Fourier transform $\lim_{T \rightarrow \infty} \int_{-T}^T dt \exp(i\omega t) \langle \psi_0 | \psi_t \rangle$ from which the eigenvalues are obtained, and

$$\langle \Gamma | \psi_E \rangle \propto \lim_{T \rightarrow \infty} \frac{1}{2T} \int_{-T}^T dt e^{iEt/\hbar} \langle \Gamma | \psi_t \rangle,$$

which gives the eigenfunctions.

The numerical propagation of a phase-space function is carried out by a split-operator method which approximates the propagator in the form

$$e^{-i\Delta t \hat{H}/\hbar} \approx \exp \left[-\frac{i\Delta t}{4\hbar m} \left(\frac{p}{2} - i\hbar \frac{\partial}{\partial q} \right)^2 \right] \exp \left[-i \frac{\Delta t}{\hbar} V \left(\frac{q}{2} + i\hbar \frac{\partial}{\partial p} \right) \right] \exp \left[-\frac{i\Delta t}{4\hbar m} \left(\frac{p}{2} - i\hbar \frac{\partial}{\partial q} \right)^2 \right]. \quad (4)$$

This is an approximation of order $O(\Delta t^3)$. Although seemingly difficult to apply, this is actually a very convenient expression since a fast-Fourier-transform routine can be utilized to evaluate the action of this operator on a function of p and q [1,2].

The diagonal matrix element of the quantum probability conservation equation is

$$\begin{aligned} \frac{\partial}{\partial t} \langle \Gamma | \hat{\rho} | \Gamma \rangle &= -\frac{\partial}{\partial q} \frac{1}{2m} [\langle \Gamma | \hat{P} \hat{\rho} | \Gamma \rangle + \langle \Gamma | \hat{\rho} \hat{P} | \Gamma \rangle] \\ &+ \frac{\partial}{\partial p} \left[\sum_{n=M}^1 V_{-n} \sum_{l=1}^n \langle \Gamma | \hat{Q}^{-l} \hat{\rho} \hat{Q}^{-n+l-1} | \Gamma \rangle \right. \\ &\left. + \sum_{n=1}^{\infty} V_n \sum_{l=0}^{n-1} \langle \Gamma | \hat{Q}^l \hat{\rho} \hat{Q}^{n-l-1} | \Gamma \rangle \right], \quad (5) \end{aligned}$$

where $\hat{\rho} = |\psi\rangle\langle\psi|$ is the time-dependent density operator and where we have assumed that the potential function can be written as $V(q) = \sum_{n=-M}^{\infty} V_n q^n$, for some positive integer M . We note that the classical limit of the above equation can be discussed only when we use an explicit solution $\hat{\rho}$. Also, we note that the above equation is a combination of the corresponding equations in coordinate,

$$\frac{\partial}{\partial t} \langle q | \hat{\rho} | q \rangle = -\frac{\partial}{\partial q} \frac{1}{2m} [\langle q | \hat{P} \hat{\rho} | q \rangle + \langle q | \hat{\rho} \hat{P} | q \rangle],$$

and momentum

$$\begin{aligned} \frac{\partial}{\partial t} \langle p | \hat{\rho} | p \rangle &= \frac{\partial}{\partial p} \left[\sum_{n=M}^1 V_{-n} \sum_{l=1}^n \langle p | \hat{Q}^{-l} \hat{\rho} \hat{Q}^{-n+l-1} | p \rangle \right. \\ &\left. + \sum_{n=1}^{\infty} V_n \sum_{l=0}^{n-1} \langle p | \hat{Q}^l \hat{\rho} \hat{Q}^{n-l-1} | p \rangle \right] \end{aligned}$$

spaces, providing a description of quantum dynamics with both variables, p and q .

The normalized phase-space density $\rho_{\psi}(\Gamma) = |\psi(\Gamma)|^2$ is proportional to the probability of finding the system in the state $|\Gamma\rangle$ which is a member of a complete set of (unnormalized) states parametrized by q and p generally characterized as coherent states [5]. Each set of generalized coherent states gives rise to a phase-space representation. However, the resemblance between the resulting phase-space density and a classical probability density strongly depends on the choice of coherent states. Here we choose $|\Gamma\rangle$ to be proportional to a minimum-uncertainty state $|\phi_{p,q}\rangle$, where $q = \langle \hat{Q} \rangle_{\phi_{p,q}}$, $p = \langle \hat{P} \rangle_{\phi_{p,q}}$, and with equal widths in the coordinate and momentum directions (in dimensionless units).

Hence, we work with a phase-space representation where the wave function is defined as

$$\psi(\Gamma) = \frac{\langle \phi_{p,q} | \psi \rangle}{\sqrt{2\pi\hbar}}. \quad (6)$$

In this representation the square magnitude of the wave function has a simple interpretation, namely, as the probability, divided by $2\pi\hbar$, of finding the system inside a phase-space volume $\delta p \delta q = 2\pi\hbar$ around the point (p, q) . Thus the quantum phase-space density constructed in this way is the one closest to a classical phase-space probability density allowed by the uncertainty principle. Furthermore, by choosing the minimum-uncertainty state to have equal uncertainties in the coordinate and momentum directions, phase space is probed isotropically. Therefore snapshots of the phase-space density

at different times give qualitative information about the location of the quantum state in phase space.

Quantitative information can be obtained, for instance, in terms of the correlation function $C(t) = |\langle \phi_{p',q'} | \psi(t) \rangle|^2$ by measuring the height of the phase-space density at the point (p', q') as a function of time. Or, the expectation values and the uncertainties of the coordinate and momentum can be calculated from the ‘‘classical-like’’ formulas [5],

$$\langle \hat{X} \rangle_{\psi} = \int d\Gamma x \rho_{\psi}(\Gamma), \quad (7)$$

$$\langle \hat{X}^2 \rangle_{\psi} = \int d\Gamma x^2 \rho_{\psi}(\Gamma) - \gamma^{\mp 2} \frac{\hbar}{2}, \quad (8)$$

where $\hat{X} = \hat{Q}, \hat{P}$ and $x = q, p$.

For our numerical studies we follow the dynamics of a system which initially is in a minimum-uncertainty state centered at (p_0, q_0) . Thus

$$\psi(\Gamma, 0) = \frac{1}{\sqrt{2\pi\hbar}} e^{-\lambda^2(q-q_0)^2/4\hbar - \lambda^{-2}(p-p_0)^2/4\hbar + i(qp_0 - pq_0)/2\hbar}, \quad (9)$$

which gives rise to the density

$$\rho_{\psi}(\Gamma, 0) = \frac{1}{2\pi\hbar} e^{-\lambda^2(q-q_0)^2/2\hbar - \lambda^{-2}(p-p_0)^2/2\hbar}, \quad (10)$$

where, again, λ is equal to unity in dimensionless units. That this density represents a minimum-uncertainty state with the desired properties can easily be verified using Eqs. (7) and (8).

To lowest order in \hbar , the probability current for the center of this density is [see Eq. (5)]

$$\begin{aligned} J_q(p_0, q_0) &= \frac{1}{2m} [\langle \Gamma | \hat{P} \hat{\rho} | \Gamma \rangle + \langle \Gamma | \hat{\rho} \hat{P} | \Gamma \rangle] \\ &= \frac{p_0}{m} \rho_{\psi}(p_0, q_0), \\ J_p(p_0, q_0) &= - \sum_{n=1}^{\infty} V_n \sum_{l=0}^{n-1} \langle \Gamma | \hat{Q}^l \hat{\rho} \hat{Q}^{n-l-1} | \Gamma \rangle \\ &= \left[F(q_0) - \lambda^{-2} \frac{\hbar^2}{2} \sum_{n=0}^{\infty} V_{n+3} J_{p,n+3} q_0^n \right] \rho_{\psi}(p_0, q_0), \end{aligned}$$

where $J_{p,n+1} = \sum_{l=0}^{n-2} l(l+1)$. Thus, for a vanishing \hbar or in potentials which are at most quadratic, the center of the density will evolve according to classical dynamics, as one would expect.

It should be noted that the classical density, Eq. (1), and the quantum density, Eq. (10), are not identical. Nevertheless, they share the same properties when calculated in the proper phase space and in that sense they represent the same state. In fact, the classical density, Eq. (1), is identical to the Wigner density corresponding to a minimum-uncertainty state [13]. However, since the Wigner density cannot, in general, be given a probabilistic interpretation we prefer to carry out our numerical investigations and comparisons in a phase

space based on projections onto minimum-uncertainty states rather than Wigner phase space since it enables us to extract qualitative information from snapshots of the phase-space density as explained above.

Furthermore, we shall see (cf. Figs. 6 and 10) that if we represent a quantum eigenstate with the energy E_n in classical phase space by a stationary solution of the classical Liouville equation of the form

$$\rho(p, q) = N e^{-[E_n - H(p, q)]^2/\sigma},$$

which has the classical average value of the energy E_n , precisely, the phase-space density in the coherent-state representation shows a much closer resemblance to this ‘‘classical analog’’ than does the Wigner density. Similar comparisons are found in Ref. [9].

In the following we present our results of propagating the function Eq. (9) and the classical Gaussian density Eq. (1) in time. All results are presented in dimensionless units and for \hbar equal to unity.

III. QUARTIC POTENTIAL

Let us consider a minimum-uncertainty wave packet, Eq. (9), moving on the potential $U(q) = q^4/4 - 4q^2$. For this potential, a classical particle can move in any of four regions: it can move along the separatrix, or it can move around any of the two minima of the potential at $q = \pm 2\sqrt{2}$, or it can move around the two of them and of the separatrix when its energy is large enough. The separatrix which separates these types of motion is given by $p^2 + q^4/2 - 8q^2 = 0$.

In Fig. 1 we show by means of density plots, in which darker regions indicate larger values of the density, the quantum evolution in phase space of the square magnitude of the minimum-uncertainty function Eq. (9) initially centered on the separatrix at $(p, q) = (3.933, -1.5)$. In all of the density plots we will show, the heights increase as a power of 1.5 in order to show the parts with a small density value, with a lowest of 0.032 of the maximum height. We can see that the probability density moves on the separatrix, and that when one part of the density is near another part of itself, some interference appears, facilitating the passage of probability through that region (these regions are pointed at with arrows). These interferences cause a perturbation on the periodicity of the motion of the density because, unexpectedly, some probability can jump back and forth between different parts of itself.

In Fig. 2 we show the evolution of $C(t) = |\langle \phi | \psi(t) \rangle|^2$ with $|\phi\rangle$ being the minimum-uncertainty state centered at $(p, q) = (6, 3)$, which is shown by the ellipse in Fig. 1(a). In that figure, there is a plot of its classical counterpart $\overline{g(t)} = \int g(p, q) \rho(p, q; t) dp dq$, where $g(p, q)$ is also a Gaussian function Eq. (1), centered at $(p, q) = (6, 3)$, and which is also acting as a probe function, but now in classical space. For the classical calculation, the initial density $\rho(p, q; t=0)$ is a Gaussian density Eq. (1) centered initially on the same point on the separatrix as the quantum one, and the propagation is governed by the classical Liouville equation. The classical average $\overline{g(t)}$ has peaks at regular periods in time and approaches a constant value because, with each oscillation, the density is slowly spreading around the separatrix (see Fig. 3).

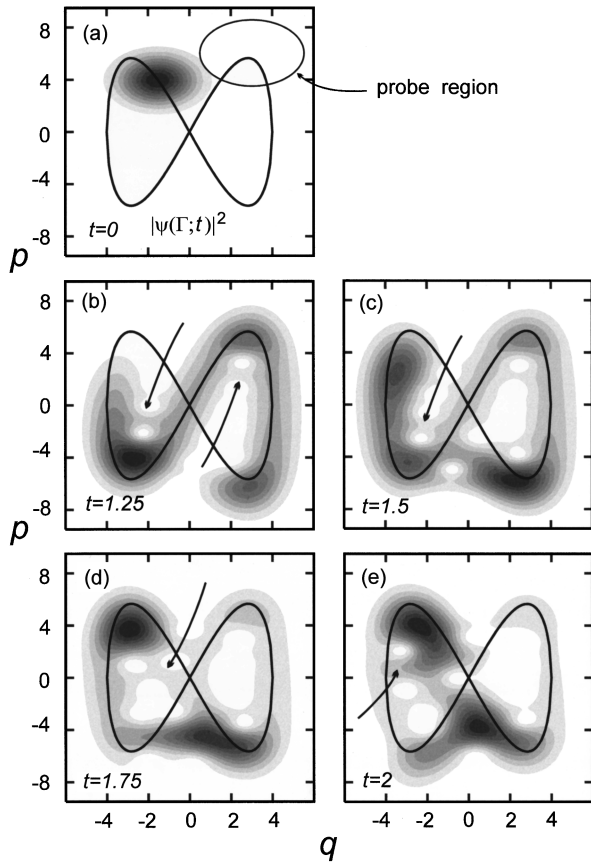


FIG. 1. Snapshots of the quantum evolution in phase space of a minimum-uncertainty function moving in a quartic potential. The initial density was centered on the separatrix.

In contrast with the quantum evolution, the classical density is mainly off the separatrix. The quantum overlap $|\langle \phi | \psi(t) \rangle|^2$ shows the effects of interference which breaks the periodic peaks we found in the classical calculation. These peaks can be identified with probability either coming from the original density or from interference. Due to this interference, quantum dynamics becomes rapidly complicated.

In Fig. 4 we show the final quantum and classical densities after propagation for a time of $t=2$, when both densities were initially centered at the bottom of the left well, at $(p, q) = (0, -2\sqrt{2})$. This time, even though part of the phase

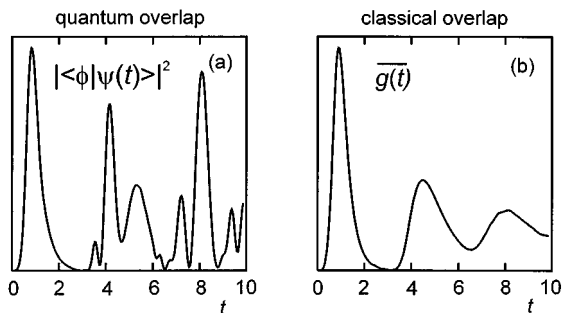


FIG. 2. Quantum and classical overlaps with a probe state for the quartic potential. The initial densities were centered on the separatrix.

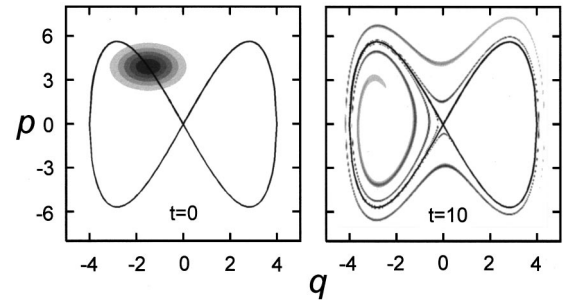


FIG. 3. Classical evolution of a Gaussian density moving in the quartic potential. The initial density was centered on the separatrix.

functions lies on and outside the separatrix, the quantum density does not escape from the well [see Fig. 4(a)] and the motion is almost periodic, as is shown by the plot of the overlap $|\langle \phi | \psi \rangle|^2$ [see Fig. 4(c)]. The probe function is also a coherent state centered at the bottom of the well as is indicated by the ellipse in Fig. 4(a). In Fig. 4(b) we can see the final classical density, which was divided by the separatrix into three parts. One of the parts evolves inside the left well, another part moves along the separatrix, and a last part travels outside the separatrix. We observe that the quantum density does not break into the pieces as the classical density does, inhibiting motion outside the well.

Other common quantities used in the analysis of the dynamics of quantum systems are $\Delta \hat{Q} = \sqrt{\langle \hat{Q}^2 \rangle - \langle \hat{Q} \rangle^2}$ and $\langle \hat{Q} \rangle$ [14]. In Fig. 5 there are plots of these quantities and of their classical counterparts $\Delta q = \sqrt{q^2 - \bar{q}^2}$, all for the propagation of Fig. 1, when the initial densities were centered on the separatrix. For short times, these classical and quantum quantities evolve in the same way. Initially, the classical density is localized in the left well and, as it moves, part of it

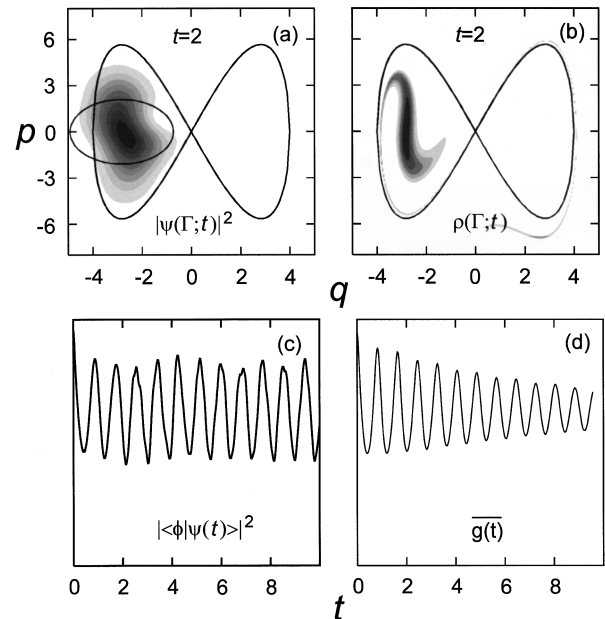


FIG. 4. Snapshots of quantum and classical evolution in the quartic potential. (a) Quantum and (b) classical densities after evolving for a time $t=2$. (c) Quantum and (d) classical overlaps. The initial densities were centered on the left bottom of the potential.

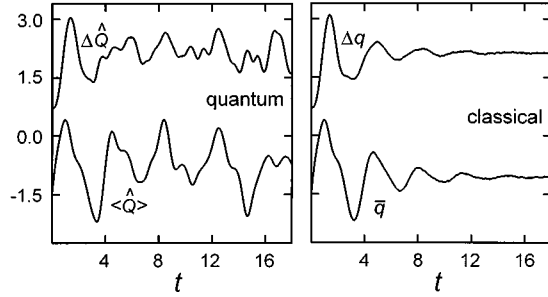


FIG. 5. Evolution of $\Delta\hat{Q}$, $\langle\hat{Q}\rangle$, Δq , and of \bar{q} for the quartic potential and when the initial density was centered on the separatrix.

separates and is distributed inside and outside the wells but most of it oscillates around the bottom of the left well. For this reason, we observe that the classical quantities decrease their variations, reaching an almost constant value. The quantum density interferes with itself trying to avoid the “stringlike” form that the classical density takes. The initial behavior observed in these quantities is independent of the specific potential in which the evolution takes place, as we will see below.

The eigenvalues closest to the energy of a classical particle on the separatrix ($E=0$) are $E=1.161\,677\,86$ and $E=-0.843\,574\,265$, to which corresponds the eigenfunctions shown in Figs. 6(a) and 6(d), respectively. Most of the probability is found near $(p,q)=(0,0)$, but a small part (with values around 0.032 of the maximum value) is found on the separatrix and on regions of phase space which were identified previously as interference regions. For comparison purposes, in Figs. 6(b) and 6(e) there are density plots of the corresponding Wigner functions. Besides being negative in some regions in phase space, the Wigner function is not large at the separatrix but in many other regions not related to it or to other classical orbits. In Figs. 6(c) and 6(f) there are density plots of the function

$$\rho(p,q) = N e^{-[E_n - H(p,q)]^2/\sigma},$$

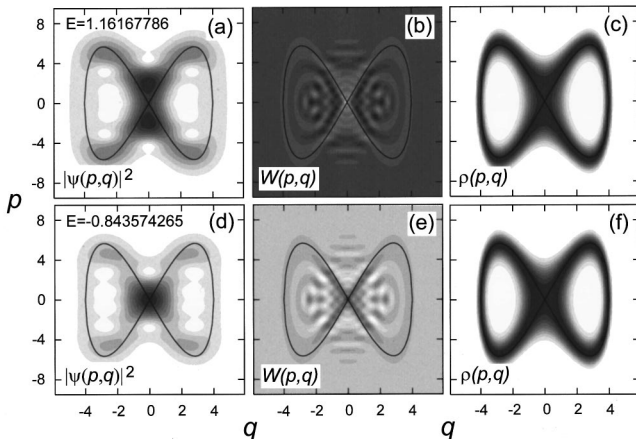


FIG. 6. Eigenfunctions with eigenvalue close to the energy ($E=0$) of a classical particle on the separatrix for the quartic potential. (a) Phase space function, (b) Wigner function, and (c) classical analog for the eigenenergy $E_n=1.161\,677\,86$ and similar plots for the eigenenergy $E=-0.843\,574\,265$ in (d), (e), and (f).

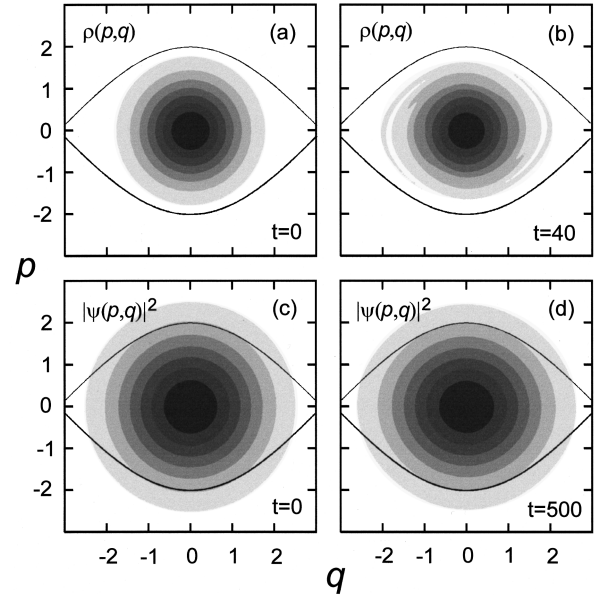


FIG. 7. Classical and quantum evolution on the pendulum potential. (a) Initial classical density centered at $(p_0, q_0)=(0,0)$; (b) classical density at time $t=40$. Quantum densities at time (c) $t=0$ and (d) $t=500$.

where N is a normalization constant, E_n is one of the quantum eigenvalues, and $H(p,q)$ is the Hamiltonian. It is seen that the densities in the coherent-state representation, Figs. 6(a) and 6(d), look more like this “classical analog” than the Wigner densities do.

IV. THE PENDULUM

In this case, the potential is $V(q)=\cos q$ and the separatrix delimits regions of confined and nonconfined motion. In Fig. 7(a) the initial classical density, centered at $(p_0, q_0)=(0,0)$, is shown. This density lies mainly inside the separatrices, and it will remain inside, redistributing in that region as time goes on, as can be seen in Fig. 7(b), where a snapshot of the classical density at time $t=40$ can be observed. In Fig. 7(c), a snapshot of the initial quantum density, which is also centered at the origin, is shown, and in Fig. 7(d), we can see the quantum density at time $t=500$. Even though part of the quantum density lies outside the separatrices, the density tends to stay together around the origin, changing its shape just a little bit. So, the well at the origin and the density itself are attractors for the quantum density not allowing it to escape.

In another evolution set, in Fig. 8(a), we can see the initial classical density centered at $(p_0, q_0)=(0, \pi)$. In Fig. 8(b), a snapshot of the classical density at time $t=13$ is shown. This time, the separatrix has divided the density at time $t=0$ into five parts. There are parts of the density which lie on regions of confined motion and remain in them, redistributing in those regions as time goes on. There is the part which lies on the separatrix, and the rest of the density moves away from where it initially started to move. In these plots, only the region of positive q is shown. In Figs. 8(c) and 8(d), snapshots of the quantum densities at times $t=0, 13$ are shown. We also find something quite different from the classical densities in Figs. 8(a) and 8(b). In this case, the quantum

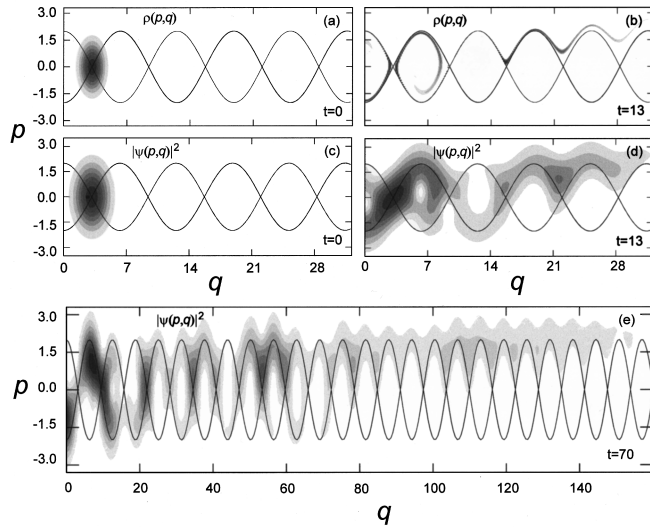


FIG. 8. Classical and quantum evolution on the pendulum potential. (a) Initial classical density centered at $(p_0, q_0) = (0, \pi)$; (b) classical density at time $t = 13$. Quantum density at times (c) $t = 0$, (d) $t = 13$, and (e) $t = 70$.

density actually moves down the separatrix, reaching regions of phase space which cannot be explored by the classical analog. In Fig. 8(e) there is a snapshot of the quantum density after a long propagation time of $t = 70$. The influence of the separatrix on the motion of the quantum density is really strong.

The evolution of the quantum $\Delta\hat{Q}$, $\langle\hat{Q}\rangle$ and classical Δq and \bar{q} quantities are shown in Fig. 9 for the cases analyzed in Figs. 7, 8. The upper two plots in Fig. 9 show the time dependency of $\Delta\hat{Q}$ and Δq when the initial densities are centered at $(p_0, q_0) = (0, 0)$, at the bottom of one of the po-

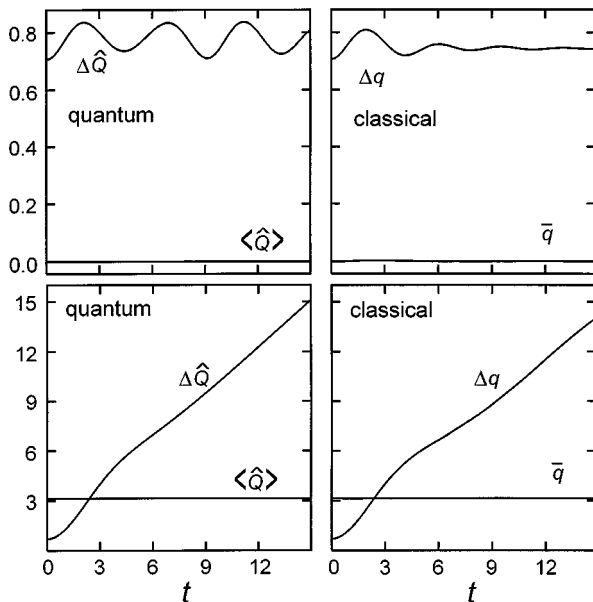


FIG. 9. Evolution of $\Delta\hat{Q}$, $\langle\hat{Q}\rangle$, Δq , and \bar{q} for the pendulum. For the upper plots, the densities were initially centered at $(p_0, q_0) = (0, 0)$, whereas for the lower ones the densities were initially centered at $(p_0, q_0) = (0, \pi)$.

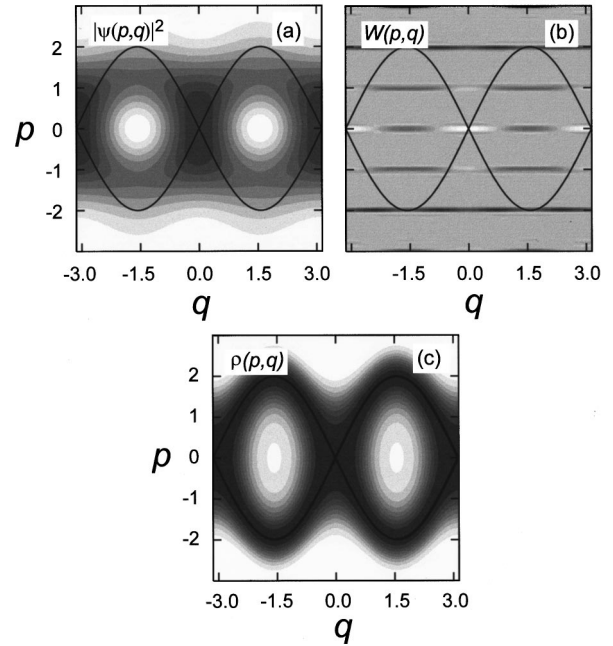


FIG. 10. Eigenfunction with eigenvalue closest to the energy of a particle on the separatrix for the pendulum potential. (a) Phase function, (b) Wigner function, and (c) classical analog.

tential wells. From the behavior of $\Delta\hat{Q}$, we can say that the quantum density expands and squeezes in the q direction in a quasiperiodic way, whereas the classical density redistributes in the well leading to an almost constant value of Δq . When the initial densities are initially centered at $(p_0, q_0) = (0, \pi)$ (lower two plots in Fig. 9), the quantum and classical quantities $\Delta\hat{Q}$ and Δq evolve in a very similar manner and, for long times, they evolve almost as for a free particle system. In any case, when the evolution begins, there is a delay in the spreading followed by an increase which resembles a trigonometric function. This time dependence is similar to the one found for the quartic potential and in other chaotic systems [14].

There is one of the eigenvalues, $E = 1.859\,108\,91$, which is the closest to the energy of a particle on the separatrix, $E = 2$. The phase-space density for this eigenenergy [see Fig. 10(a)], together with the Wigner function [see Fig. 10(b)], and the ‘‘classical analog’’ $\rho(p, q) = N \exp\{-[E_n - H(p, q)]^2/\sigma\}$ [see Fig. 10(c)], are shown in Fig. 10. The phase-space density has a large probability around where the separatrix touches the hyperbolic point, and in the interference regions which allow the probability to jump between different parts of the density. The classical analog lies almost on the separatrix and it also has a large probability around the hyperbolic points. The Wigner function has no resemblance to any classical trajectory at all.

V. THE KICKED HARMONIC OSCILLATOR

So far we have only considered regular systems and the question now is if the same type of behavior is found in nonregular ones. Then, we now turn our attention to the kicked harmonic oscillator model with mapping [15,16]

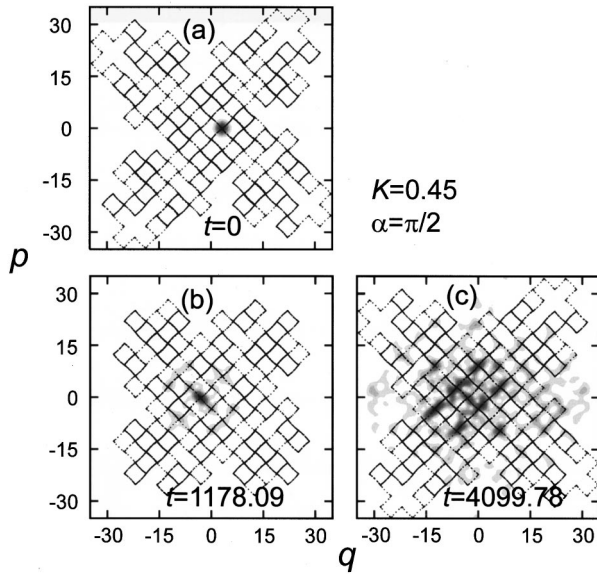


FIG. 11. Quantum evolution in the kicked harmonic oscillator map, for $K=0.45$ and $\alpha=\pi/2$. (a) Initial density centered at $(p_0, q_0)=(0, 2\pi)$. Densities at times (b) 1178.09 and (c) 4099.78.

$$\begin{aligned}
 p_{n+1} &= (p_n + K \sin q_n) \cos \alpha - q_n \sin \alpha, \\
 q_{n+1} &= (p_n + K \sin q_n) \sin \alpha + q_n \cos \alpha.
 \end{aligned}
 \quad (11)$$

In this system, there is a stochastic web in phase space which depends upon the values of the constants K and α .

In Fig. 11, we show the result of a numerical quantum propagation of the phase-space minimum-uncertainty function, Eq. (9) in this system. Parts of the stochastic web and density plots of the quantum density $|\psi(\Gamma; t)|^2$ for $K=0.45$ and $\alpha=\pi/2$, at different times, are shown. The minimum-uncertainty function, Eq. (9), was initially centered at $(p_0, q_0)=(0, 2\pi)$, i.e., at one of the intersections of the web. In the beginning of the evolution, the function spreads rather quickly on phase space, but due to interference effects and the web, it does not spread that far from the original location at which it started to move, and sometimes it almost returns to its initial form and location [see Figs. 11(b) and 11(c)]. From these numerical calculations, it is evident that the quantum system uses the stochastic web in order to disperse and redistribute around in phase space faster than its classical model, but the interference effects inhibits the spreading to regions far away from the original location.

In another propagation set (see Fig. 12), we had centered the initial function at $(p, q)=(0, 0)$, i.e., in the center of one of the regular regions. This time, the stochastic web is used by the quantum density in a different way. The density jumps from a regular region to another through the intersections of the web. The motion was periodic during the propagation, oscillating between states like the one shown in Fig. 12(b) and the one in Fig. 12(c). The density jumps four or five regions away around the original location [see Fig. 12(b)], and then it jumps back to the original site, almost recovering its original shape [see Fig. 12(c)]. Even though it seems that the phase-space density periodically almost returns to its original shape, the analysis of the small parts of the phase

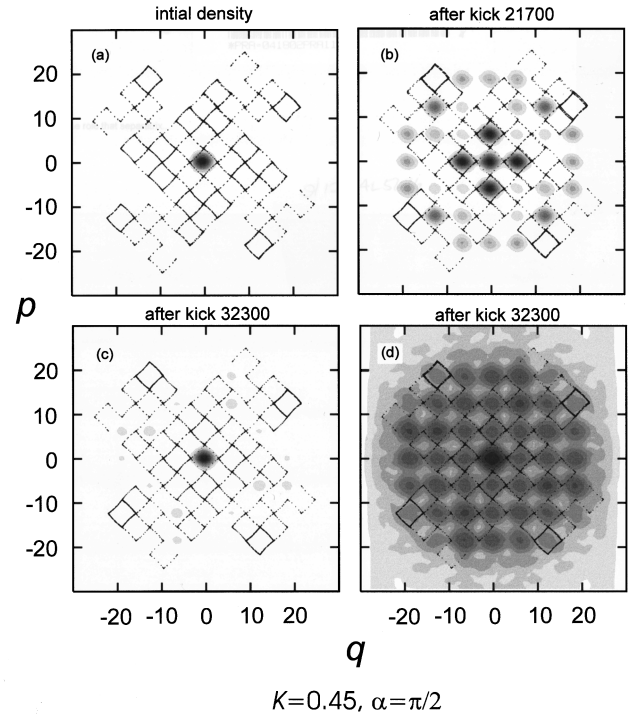


FIG. 12. Quantum evolution in the kicked harmonic oscillator map, for $K=0.45$ and $\alpha=\pi/2$. (a) Initial density centered at $(p_0, q_0)=(0, 0)$. Densities just after the (b) 21 700th and (c) 32 300th kicks. (d) is the same as (c) but showing the parts with very small probability.

density [see Fig. 12(d)] shows that it is actually distributed on a wider region, similar to that of Fig. 12(b).

The case of fivefold symmetry is shown in Fig. 13, where $K=0.2$ and $\alpha=2\pi/5$. In the first and second rows of plots, from top to bottom, the initial density was centered on two

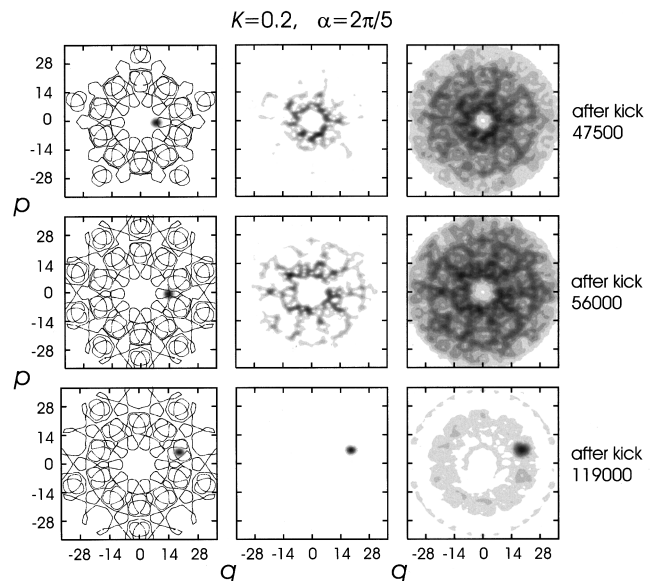


FIG. 13. Quantum evolution for the kicked harmonic oscillator map for $\alpha=2\pi/5$ and $K=0.2$. In the two upper rows of plots the densities were initially centered at two different points on the stochastic web. In the bottom row, the density was initially centered at the center of one of the regular regions.

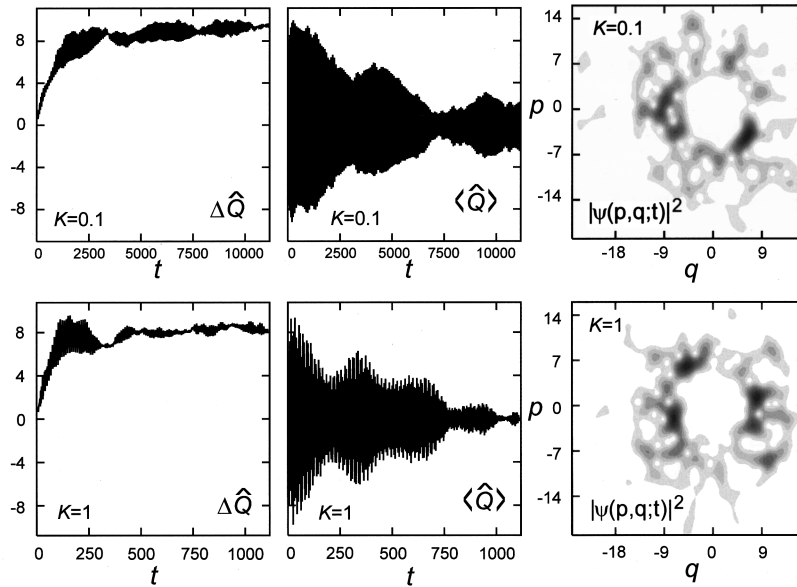


FIG. 14. Long time quantum evolution of $\Delta\hat{Q}$ and $\langle\hat{Q}\rangle$ for the kicked harmonic oscillator map for the cases $K=0.1$ (upper row of plots) and $K=1$ (lower row of plots), with $\alpha=2\pi/5$.

points on the stochastic web, whereas in the lower row it was initially centered in the middle of one of the regular regions. The left plot in each row shows the initial density, whereas middle and right plots show the final densities but with contour levels increasing as the powers 1.7 and 6, respectively. The smallest heights shown are 0.02 and 10^{-6} of the maximum height for each density. The conclusions drawn after looking at the final densities can be very different, depending on the scheme adopted to choose the heights of the contour levels. When the height of the contour levels increases as the power 1.7 (which corresponds to the plots in the middle of each row in Fig. 13) we conclude that when the quantum density is initially centered on a separatrix, it slowly redistributes itself on the web, but it does not travel too far from the “ring” where it started. Then, as time increases, the density traces and highlights part of the web. When the density is initially centered in the middle of one of the regular regions (bottom row of plots in Fig. 13), the density never abandons the region. However, when we adopt the scheme in which the height of the contour levels increases as a power 6, we find that something subtle happens (right plots in Fig. 13): very small amounts of the density actually fill a wide region in phase space, even in the case where we thought that the density was trapped in a regular region.

With the increase of K , the thickness and complexity of the stochastic web increases and the quantum density finds it easier to diffuse in phase space, as we can see in Fig. 14, in which we show plots of $\Delta\hat{Q}=\sqrt{\langle\hat{Q}^2\rangle-\langle\hat{Q}\rangle^2}$, $\langle\hat{Q}\rangle$, and $|\psi(q,p;t)|^2$ after a long propagation time corresponding to the case of the upper row of plots in Fig. 13, with the density initially centered at the same point in phase space. In the upper row of plots, $K=0.1$ and, by looking at the behavior of $\Delta\hat{Q}$, we see how the width of the wave functions increases rapidly reaching an oscillatory value around 10. The spreading of the wave function is also reflected in the values that $\langle\hat{Q}\rangle$ takes; initially the probability density is centered around the point (p_0, q_0) and starts to rotate and spread around the

origin. As the wave function is redistributed in phase space, the average $\langle\hat{Q}\rangle$ oscillates between smaller values around zero. Typically, the probability density in phase space looks like the one shown in the rightmost upper plot of Fig. 14. The behavior for larger values of K is the same one, as can be observed in the lower row of plots in Fig. 14 in which $K=1$; the behavior is the same but ten times faster compared with the behavior for $K=0.1$. However, the probability density for $K=1$ suggests the same web as for the case of $K=0.1$, even though the web is much wider, with large regions of chaotic behavior. The widening of the web enhances the process of redistribution of the wave function but this does not increase the extension that it covers; the wave function stays together and does not allow for further spreading.

For the classical system, the evolution of Δq and \bar{q} is shown in Fig. 15. Δq also increases very rapidly until it reaches values around a value which is smaller than the quantum one. The fact that the classical density does not use the separatrix to reach classically unavailable regions of phase space is reflected in the evolution of Δq and of \bar{q} which oscillates with large amplitudes.

VI. CONCLUDING REMARKS

Separatrices and stochastic webs are traveled in different ways in a quantum and classical phase space. If part of a classical system happens to lie on a separatrix or web or a regular region, it will travel on it forever, but a quantum density will use them in order to gain access to classically unreachable regions of phase space. Thus this is another mechanism, similar to that of tunneling, that distinguishes quantum evolution.

We found that, for the kicked harmonic oscillator, due to interference effects, even though the quantum density has more freedom to wander in phase space, it covers just a region in the vicinity of the initial site, inhibiting the dispersion away from it, inhibiting chaos in a classical sense.

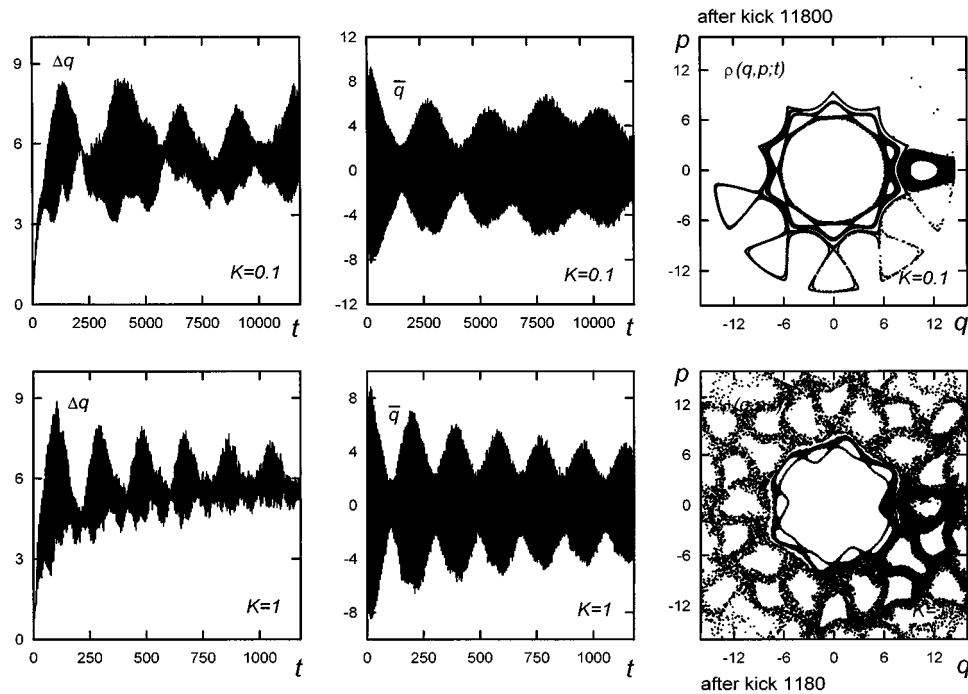


FIG. 15. Classical evolution of Δq and \bar{q} for the kicked harmonic oscillator map for the cases $K=0.1$ (upper row of plots) and $K=1$ (lower row of plots), with $\alpha=2\pi/5$.

We have found general features which apply to quantum systems, regardless of whether the system is regular or not, or the potential is continuous or not. One of these features is that since the wave function cannot be discontinuous in phase space, it becomes more rounded than its classical analog and it can break apart into pieces before it gets “too thin.” According to this, the separatrix or stochastic web does not partition the quantum density as happens in the classical case, instead it is used as a road to classically unavailable regions in phase space. The amount of the classical density which lies on the web is fixed at the initial time and only this amount diffuses through the stochastic web. The rest of the density moves in regions of regular motion. We have also found that the quantum density actually is attracted to fixed points and to separatrices and stochastic webs of the corresponding classical system.

Regardless of whether the system is integrable or not, classical or quantum, when the density spreads, $\Delta\hat{Q}$ remains

constant for a short time and then rises and oscillates, similar to a cosine function.

Finally, we can say that different information about the dynamics of quantum systems is obtained by looking at the different heights of the quantum probability density in phase space. The peaks of the density show some of the classical features, things like scars [11], whereas the zeros of the phase-space densities can be used to determine if a particular eigenstate is a regular or an irregular one [12]. In this work we have shown that the parts of probability densities with small values are also important in the elucidation of the evolution of quantum systems.

ACKNOWLEDGMENTS

We would like to acknowledge financial support from CONACyT and SNI, Mexico as well as support from the Danish Natural Science Research Council.

-
- [1] Go. Torres-Vega and J. H. Frederick, Phys. Rev. Lett. **67**, 2601 (1991); Go. Torres-Vega and J. D. Morales-Guzmán, J. Chem. Phys. **101**, 5847 (1994).
- [2] Go. Torres-Vega, J. Chem. Phys. **98**, 7040 (1993); **99**, 1824 (1993).
- [3] G. Dattoli, L. Giannessi, P. L. Ottaviani, and A. Torre, Phys. Rev. E **51**, 821 (1995).
- [4] Go. Torres-Vega and John H. Frederick, J. Chem. Phys. **93**, 8862 (1990); **98**, 3103 (1993).
- [5] K. Møller, T. G. Jørgensen, and Go. Torres-Vega, J. Chem. Phys. **106**, 7228 (1997).
- [6] K. Husimi, Proc. Phys. Math. Soc. Jpn. **22**, 749 (1940).
- [7] E. Wigner, Phys. Rev. **40**, 749 (1932); M. Hillery, R. F. O’Connell, M. O. Scully, and E. P. Wigner, Phys. Rep. **106**, 121 (1984).
- [8] A. Royer, Phys. Rev. Lett. **55**, 2745 (1985).
- [9] K. Takahashi, J. Phys. Soc. Jpn. **55**, 762 (1986).
- [10] R. T. Skodje, H. W. Rohrs, and J. VanBuskirk, Phys. Rev. A **40**, 2894 (1989).
- [11] Martin C. Gutzwiller, *Chaos in Classical and Quantum Mechanics* (Springer-Verlag, New York, 1990).
- [12] P. Leboeuff and A. Voros, J. Phys. A **23**, 1765 (1990).
- [13] In Wigner phase space the formulas corresponding to Eq. (8)

do not contain the second term on the right hand side.

- [14] Ronald F. Fox and T. C. Elston, *Phys. Rev. E* **49**, 3683 (1994).
- [15] G. P. Berman, V. Yu. Rubaev, and G. M. Zaslavsky, *Nonlinearity* **4**, 543 (1991); G. M. Zaslavskii, M. Yu. Zakharov, R. Z. Sagdeev, D. A. Usikov, and A. A. Chernikov, *Zh. Eksp. Teor.*

Fiz. **91**, 500 (1986) [*Sov. Phys. JETP* **64**, 294 (1986)].

- [16] For a review on comparisons of quantum-mechanical and classical behavior of other kicked systems, see, e.g., F. Haake, *Quantum Signatures of Chaos* (Springer, Berlin, 1991), Chap. 7.